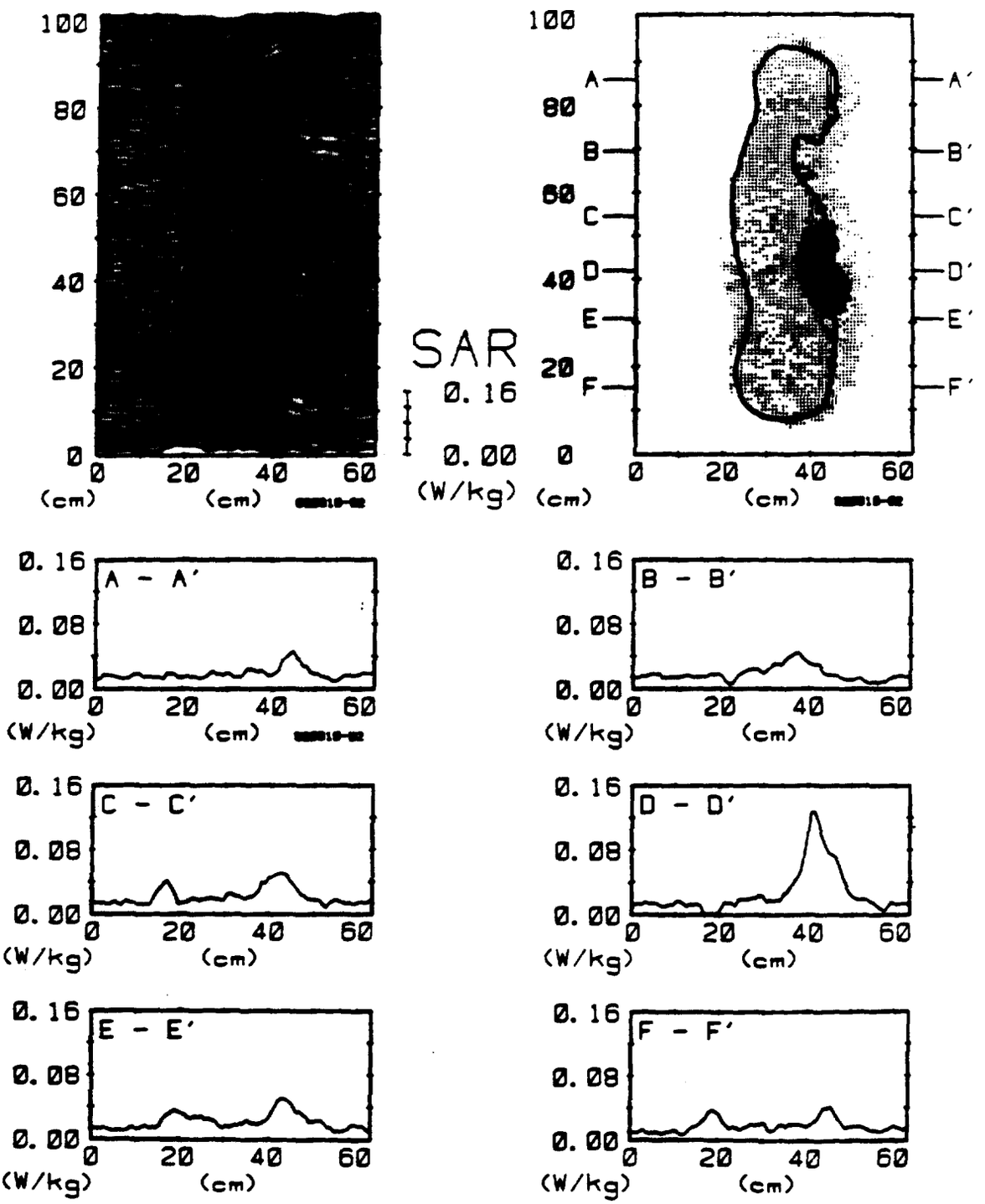

Fig. 57. Computer-processed thermograms showing SAR distribution in sagittal plane of woman model exposed to 835-MHz in standing position exterior of automobile 9.7 cm from trunk-mounted antenna with 1-W input.

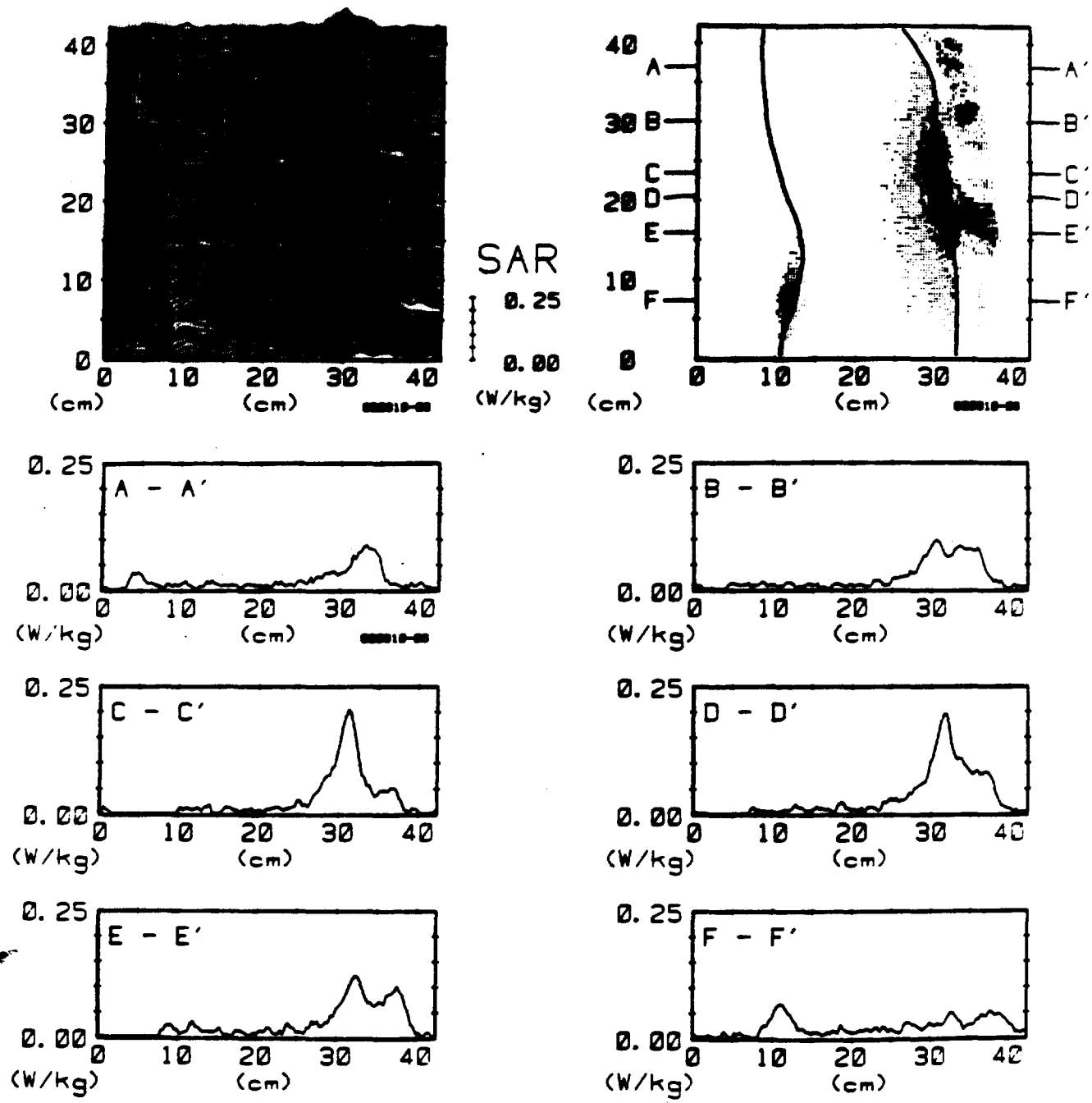

Fig. 58. Closeup thermograms showing SAR distribution in sagittal plane of woman model exposed to 835-MHz in standing position exterior of automobile 9.7 cm from trunk-mounted antenna with 1-W input.

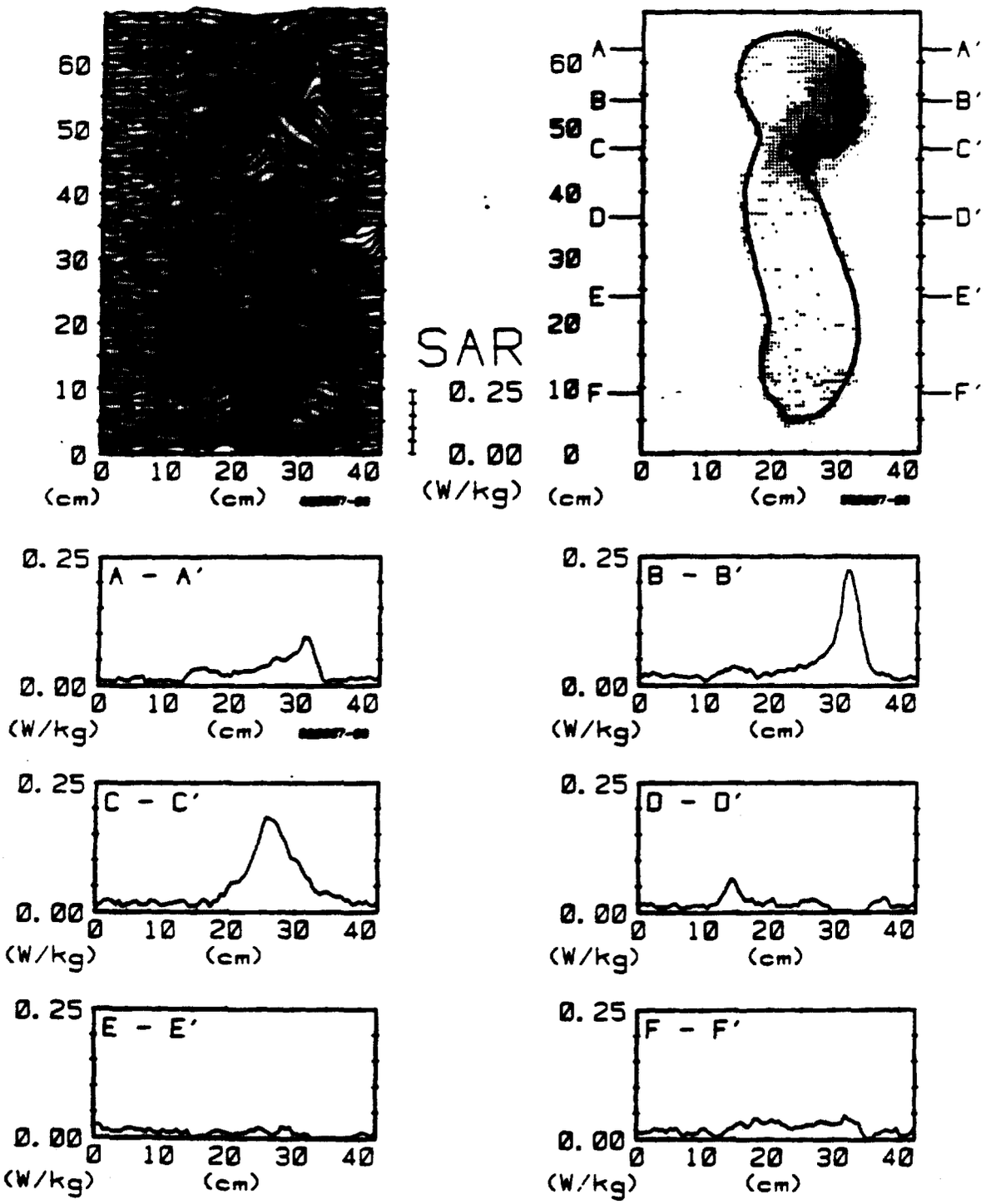

Fig. 59. Computer-processed thermograms showing SAR distribution in sagittal plane of child model exposed to 835-MHz in standing position exterior of automobile 15 cm from trunk-mounted antenna with 1-W input.

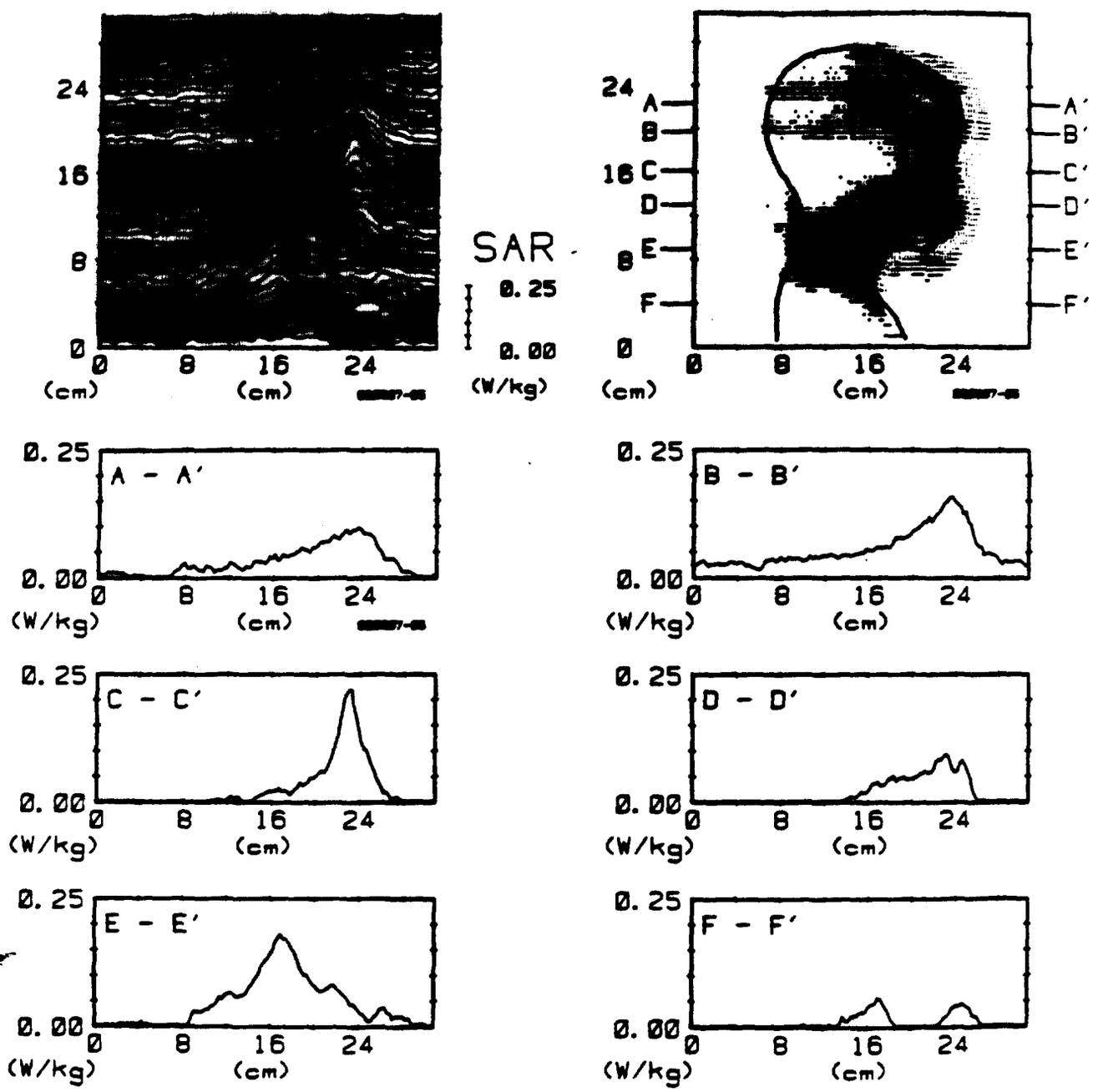

Fig. 60. Closeup thermograms showing SAR distribution in sagittal plane of child model exposed to 835-MHz in standing position exterior of autombile 20 cm from trunk-mounted antenna with 1-W input.

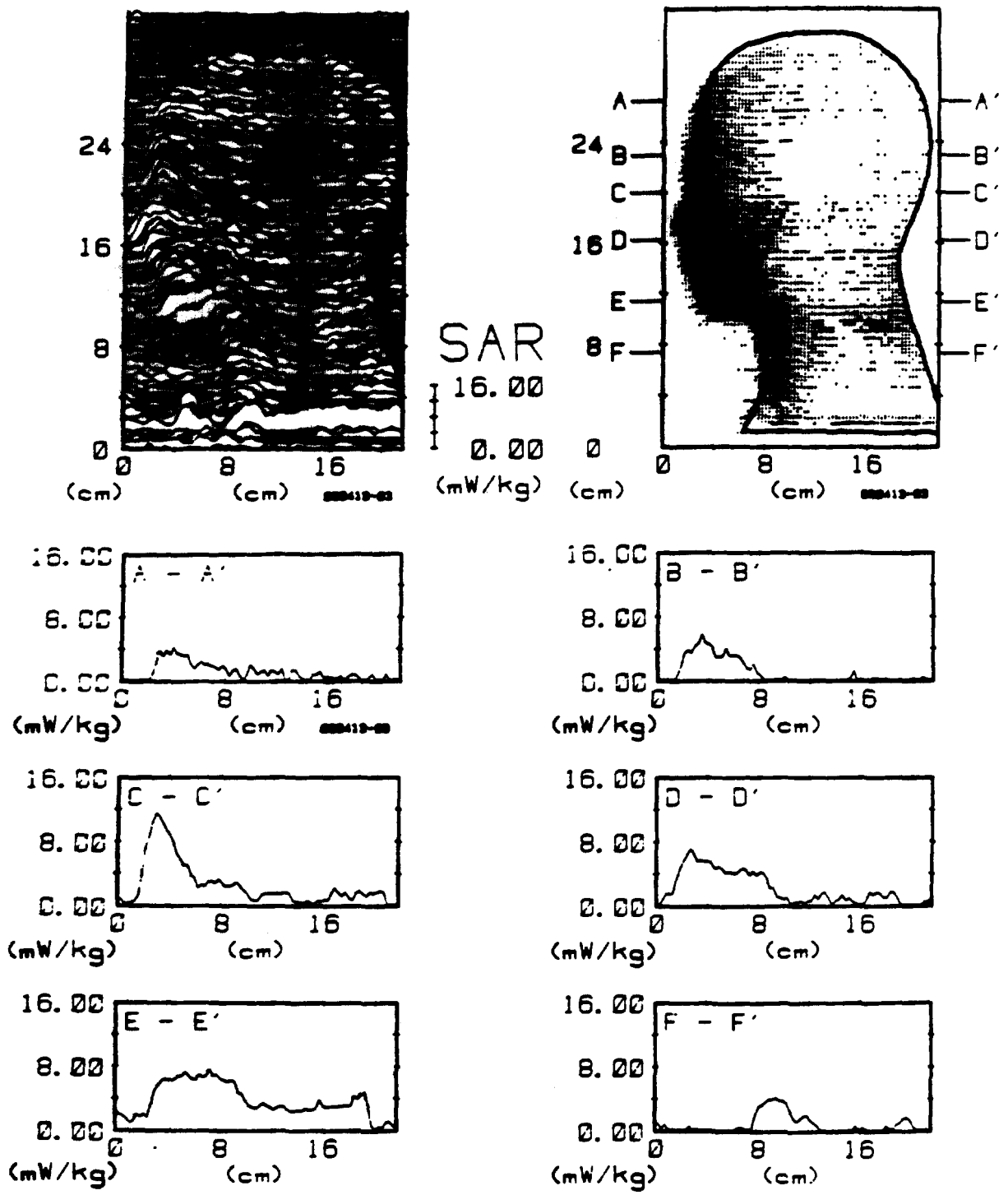

Fig. 61. Computer-processed thermograms showing SAR distribution in sagittal plane of child model exposed to 835-MHz in kneeling position interior of automobile 20 cm from trunk-mounted antenna with 1-W input.

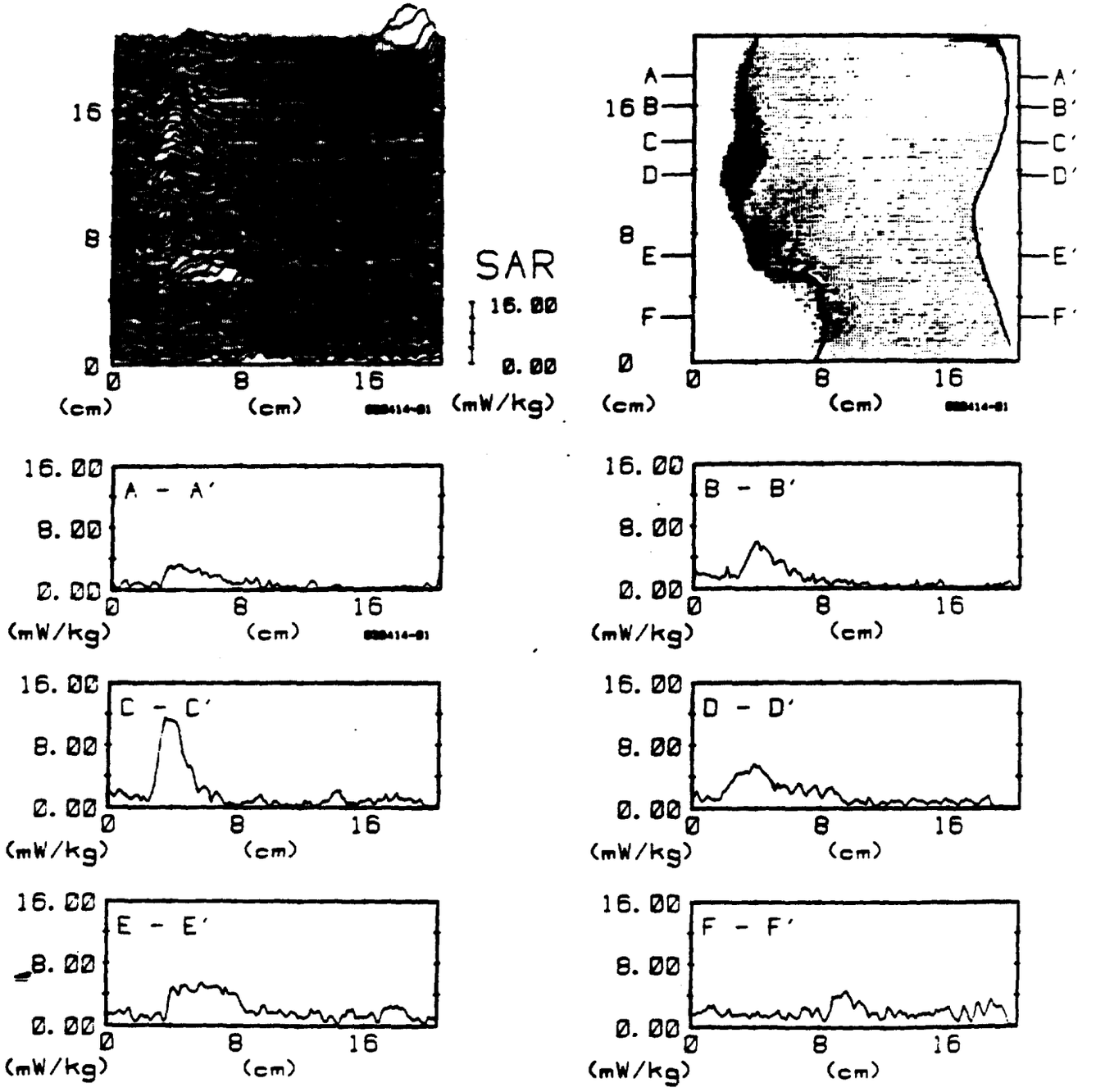

Fig. 62. Closeup thermograms showing SAR distribution in sagittal plane of child model exposed to 835-MHz in kneeling position interior of automobile 70 cm from trunk-mounted antenna with 1-W input.

the standing man and woman models exposed at 12 cm or 9.5 cm from the trunk-mounted antenna. The maximum level was at the stomach region in both models. The SARs in the breast of the woman model are tabulated in Table 9; the values are smaller than those in the stomach and liver regions. In Table 10 are given the results for the child model.

Electric-Field Measurements in Subjects Exposed in Automobile

In Figs. 63 and 64 are illustrated the maximum SARs at the surfaces of the face and neck of the child exposed in the automobile while looking out the back window. These measurements were made with the diode electric-field sensor inserted through the back of the head of the model, in contact with the internal surface of the fiberglass shell. The levels are higher than, but agree reasonably well with the values obtained thermographically for the same model, shown in Fig. 62. The thermograph results can be expected to be lower as a result of reduction in temperature from thermal diffusion prior to thermography. In Figs. 65 and 66 are illustrated the SARs over the surfaces of the back of the head and neck of the man model sitting in the back of the car exposed to the trunk-mounted antenna. The values were measured with the electric-field probe in the same manner as for the child. Maximum level at the neck of the man was 0.019 W/kg per watt input into the antenna; this value corresponds approximately to .05 W/kg per mW/cm^2 of incident power density.

TABLE 9. SARs IN BREASTS OF STANDING WOMAN MODEL EXPOSED TO TRUNK-MOUNTED ANTENNA (W/kg PER WATT)

Depth (cm)	Left (center)	Left (-2.8 cm)	Right (center)	Right (-2.8 cm)
0.5	0.0517	0.0788	0.0459	0.0864
1	0.0437	0.0643	0.0374	0.0742
2	0.0319	0.0353	0.0293	0.0500
3	0.0247	0.0203	0.0232	0.0294
4	0.0180	0.0102	0.0181	0.0199
5	0.0133	0.0054	0.0130	0.0097
6	0.0079	0.0030	0.0074	0.0042
7	0.0040	0.0017	0.0035	0.0022
8	0.0022	0.0009	0.0015	0.0009
9	0.0009	0.0005	0.0008	0.0004

TABLE 10. SARs IN HEAD AND NECK OF STANDING CHILD EXPOSED TO TRUNK-MOUNTED ANTENNA (W/kg PER WATT)

Depth (cm)	Eye		Nose		Mouth	
	Left	Right	Left	Right	Left	Right
0	0.123	0.176	0.077	0.102	0.091	0.049
1.0	0.069	0.106	0.055	0.095	0.037	0.040
2.0	0.034	0.053	0.034	0.063	0.032	0.034
4.0	0.015	0.028	0.021	0.052	0.030	0.030
5.0	0.007	0.013	0.015	0.027	0.037	0.043
6.0	0.003	0.005	0.013	0.020	0.047	0.054
7.0					0.048	0.037
8.0					0.043	0.025
9.0					0.034	0.019
10.0					0.025	0.015
11.0					0.018	0.016
12.0					0.018	0.021
13.0					0.010	0.012

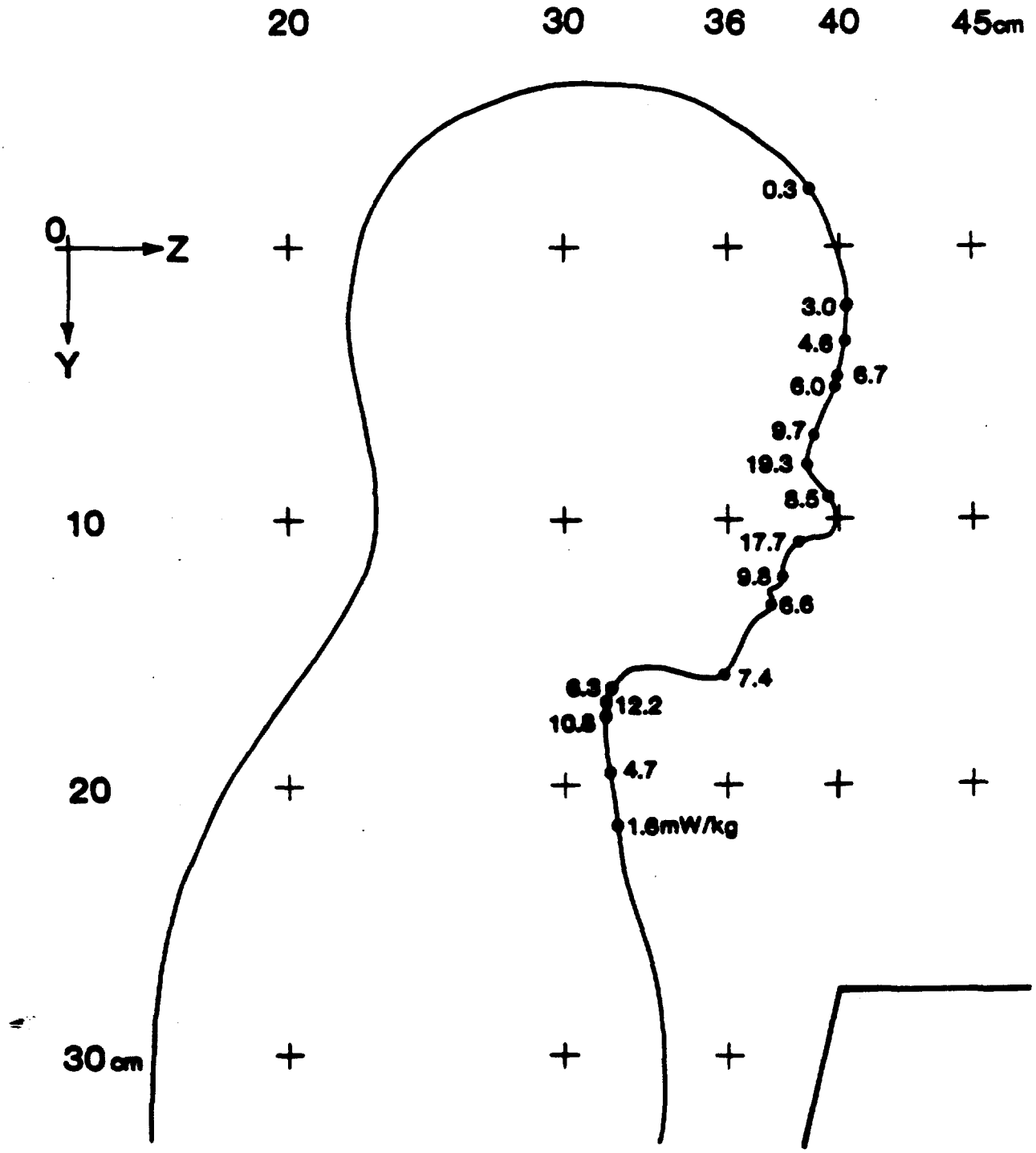

Fig. 63. Maximum SAR at the surface of the face of child model in kneeling position interior of automobile exposed to 835-MHz radiation from trunk-mounted antenna with 1-W input power (Y-Z plane, X= +20 cm).

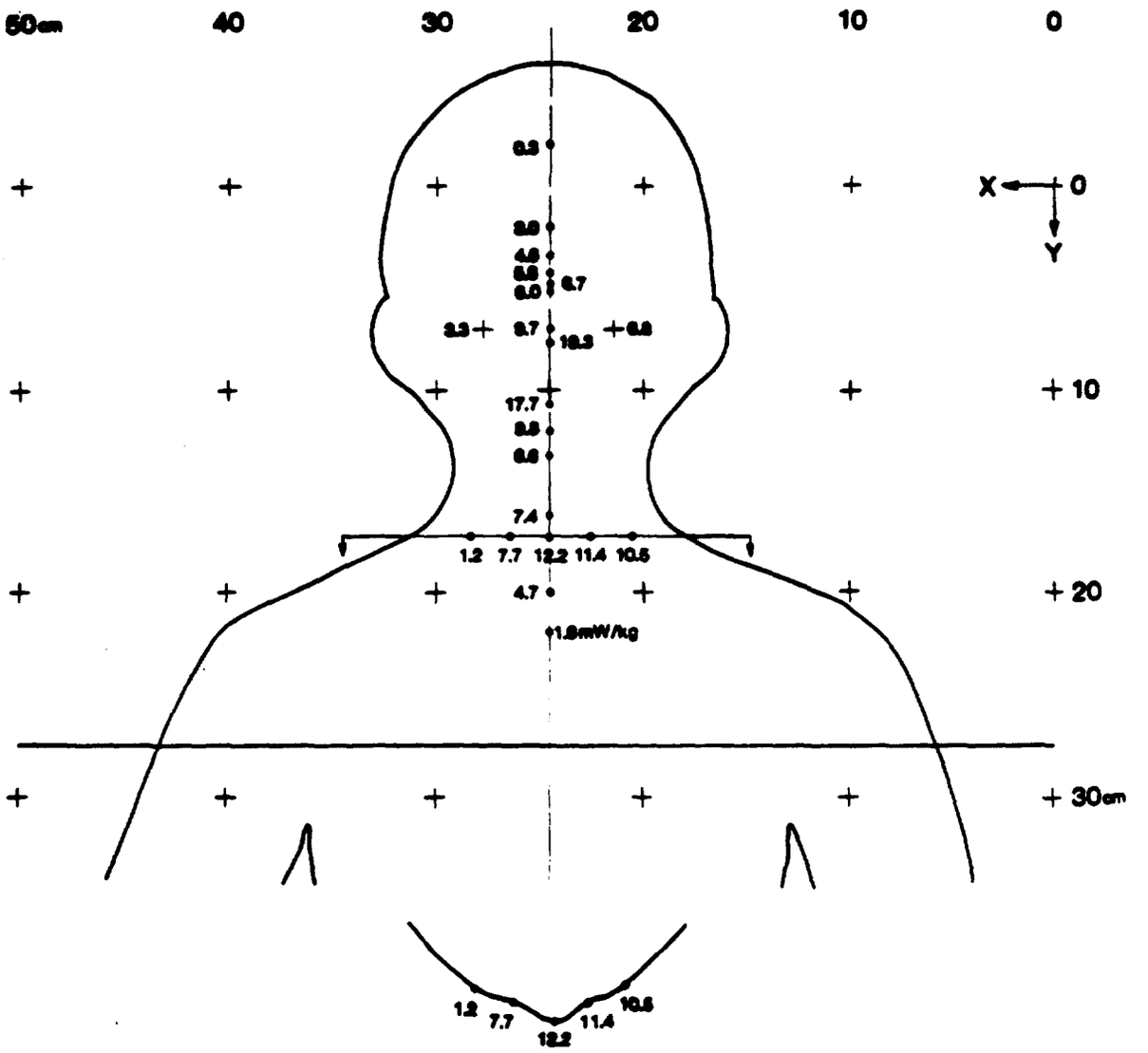

Fig. 64. Maximum SARs at the surfaces of the eye, neck, and forehead of child model in kneeling position interior of automobile exposed to 835-MHz radiation from trunk-mounted antenna with 1-W input power (X-Y plane, Z= 30 cm).

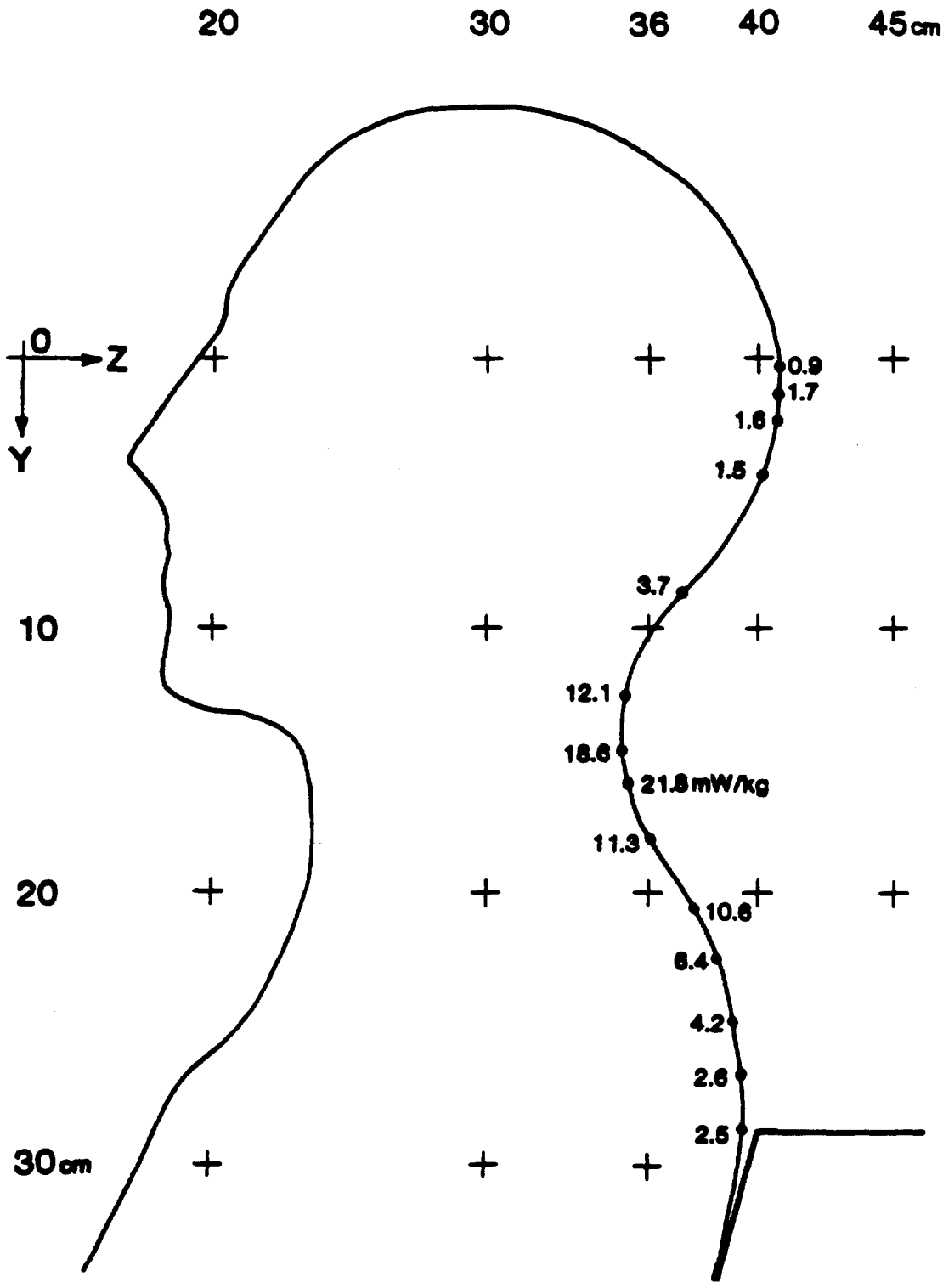

Fig. 65. Maximum SAR at the back of head surface of man model in sitting position interior of automobile exposed to 835-MHz radiation from trunk-mounted antenna with 1-W input power (Y-Z plane, X= +30 cm).

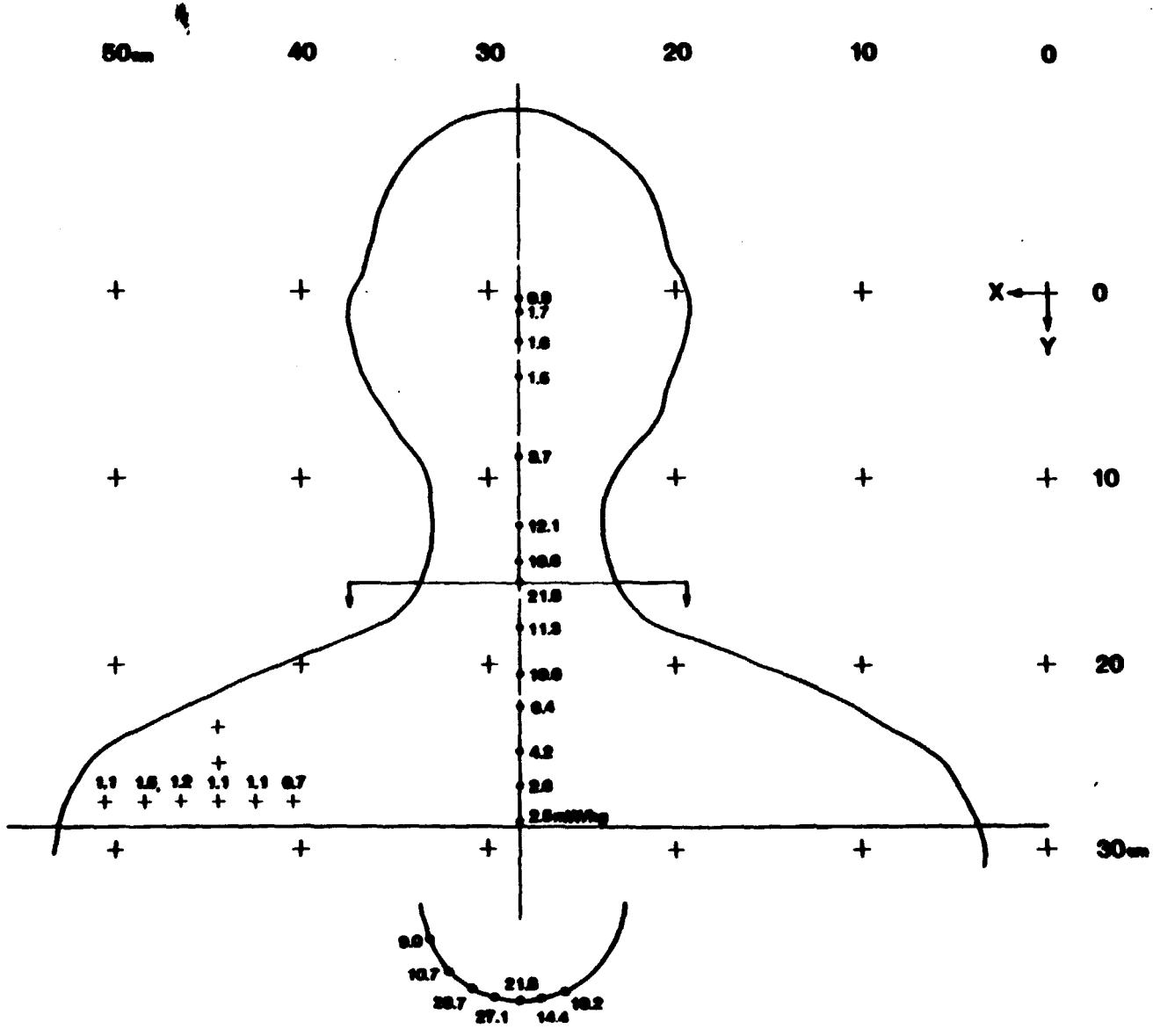

Fig. 66. Maximum SARs at the back of head, and shoulder and neck surfaces of man model in sitting position interior of automobile exposed to 835-MHz radiation from trunk-mounted antenna with 1-W input power (X-Y plane, Z= 30 cm).

4 CONCLUSIONS AND FUTURE RESEARCH

In Table 11 are summarized all of the results of the experimental measurements for maximum power density and SAR per watt into the antenna and maximum SAR per mW/cm^2 incident to the subject for the various exposure conditions tried in this research. In Table 12, column 4 are listed the maximum inputs of power that could be applied to the antenna without exceeding the maximum allowed by the ANSI C95.1, 1982 Radio Frequency Protection Guide (RFPG). The RFPG is based on limiting the whole-body average SAR to 0.4 W/kg, which is a factor of 10 below the level of 4 W/kg deemed by ANSI to be the threshold for hazardous biological effects. This threshold is for the most sensitive reported endpoint of behavioral distruption in the scientific literature that ANSI used as the basis for the RFPG.

The RFPG specifies that human exposure levels between 300 MHz and 1500 MHz should not exceed the level of $1500/f$ mW/cm^2 (where f = frequency in MHz) for whole-body average SAR not to exceed 0.4 W/kg. Thus, at 835 MHz the maximum permissible level is 2.78 mW/cm^2. It should be emphasized, however, that the level is based on whole-body exposures that would result in a total of up to 28 W absorption in a 70-kg adult. Clearly, the emission from the mobile antenna results in only partial body exposure. Application of the RFPG exposure criteria based on a maximum whole-body exposure of 2.78 mW/cm^2 would limit the input power to the antenna to 4.46 W for the condition resulting in the highest exposure level studied in this research (woman standing 9.7 cm from antenna). It is obvious, however, that under this restriction only a fraction of the 4.46 W emitted by the antenna would be absorbed by the exposed subject; thus, biologically the exposure level is much less significant than the same level for whole-body exposure. The RFPG takes into account such partial-body exposure conditions by specifiying an exclusion clause that would allow higher exposure levels provided that the localized SAR in tissue does not exceed levels possible with planewave exposures at the recommended maximum power densities. This maximum level of SAR is approximately 20 times the average, or 8 W/kg. The last column of Table 12 gives the maximum input

TABLE 11. SUMMARY OF MAXIMUM POWER DENSITIES AND SARs FOR VARIOUS EXPOSURE CONDITIONS

Antenna	Model	Position	Max Power density (mW/cm per W)	Max SAR (W/kg per W)	Max SAR (W/kg per mW/cm)
Roof	Woman	Leaning forward (43.5cm)	0.1278	0.023	0.180
Roof	Woman	Standing (63 cm)	0.0639	0.049	0.767
Roof	Child	Leaning forward (39 cm)	0.1475	0.052	0.353
Roof	Child	Standing (63 cm)	0.0639	0.019	0.297
Trunk	Man	Standing (12 cm)	0.4350	0.120	0.276
Trunk	Woman	Standing (9.7 cm)	0.6235	0.200	0.321
Trunk	Child	Standing (15 cm)	0.3567	0.230	0.645
Trunk	Man	Sitting	0.0443	0.022	0.497
Trunk	Child	Kneeling	0.0443	0.019	0.429

TABLE 12. MAXIMUM INPUT POWERS INTO ANTENNA ALLOWED BY THE ANSI C95.1, 1982 STANDARD FOR VARIOUS EXPOSURE CONDITIONS

			Maximum input power (watt)	
Antenna	Model	Position	Power density (2.78 mW/cm)	SAR (8 W/kg)
Roof	Woman	Leaning forward (43.5 cm)	21.75	348
Roof	Woman	Standing (63 cm)	43.51	163
Roof	Child	Standing (39 cm)	18.85	154
Roof	Child	Standing (63 cm)	43.51	421
Trunk	Man	Standing (12 cm)	6.39	67
Trunk	Woman	Standing (9.7 cm)	4.46	40
Trunk	Child	Standing (15 cm)	7.79	35
Trunk	Man	Sitting	62.75	364
Trunk	Child	Kneeling	62.75	421

power to the antenna for preventing the localized SAR to exceed 8 W/kg for all the exposure conditions considered in this research. Note from that table, under this exclusion criterion, that a maximum input power of 35 watts would be allowed to the antenna.

In view of the fact that the highest levels of measured local SAR occurred in the region of the eyes of an exposed child 15 cm from the antenna, some comments should be made concerning possible microwave effects on the exposed eye. The lowest thresholds for cataract formation in laboratory animals due to acute exposure to microwave radiation are more than 10 times above the maximum localized exposure and SAR levels allowed by the ANSI RFPG (requiring 50 to 100 min of exposure) at 150 to 500 mW/cm^2, corresponding to a localized SAR of 130 to 435 W/kg (Carpenter et al. 1974; Guy et al. 1975; Kramar et al. 1975). Also, it has been demonstrated that chronic exposure of rabbits for up to 6 months in duration to 10 mW/cm^2 maximum (SAR = 17 W/kg) failed to produce any cataracts (Guy et al. 1980). It should be noted that the above experiments were conducted with rabbits, whose eyes protrude from the head, and thus are more susceptible to microwave damage. Similar experiments on monkeys, which more closely represent the humans species, failed to produce cataracts at exposure levels as high as 150 to 500 mW/cm^2 (Kramar et al. 1978; McAffee et al. 1979).

The ANSI RFPG and other forthcoming exposure guides exempt devices with less than 7-W input power to the antenna. The maximum power densities and SARs for all of the exposure conditions tested with this input power to the antenna are tabulated in Table 13. As can be seen, the worst exposure condition does not satisfy the ANSI primary exposure criteria; however, it does satisfy the 7-W and 8-W/kg exclusion clauses. On the other hand, a maximum input power of 3.5 W would satisfy all of the ANSI guides, as shown in Table 14.

It is of interest to compare the maximum measured values of power density for different distances with the theoretical values from an equivalent half-wavelength-long dipole. Calculations of the field strength and power density based on the equations for the infinitesimally thin

TABLE 13. SUMMARY OF MAXIMUM POWER DENSITIES AND SARs CORRESPONDING TO 7-W INPUT POWER TO ANTENNA FOR VARIOUS EXPOSURE CONDITIONS

Anetnna	Model	Position	Max Power density (mW/cm^2)	Max SAR (W/kg)
Roof	Woman	Leaning forward (43.5 cm)	.895	.161
Roof	Woman	Standing (63 cm)	.447	.343
Roof	Child	Leaning forward (39 cm)	1.03	.364
Roof	Child	Standing (63 cm)	.447	.133
Trunk	Man	Standing (12 cm)	3.05	.840
Trunk	Woman	Standing (9.7 cm)	4.36	1.40
Trunk	Child	Standing (15 cm)	2.50	1.61
Trunk	Man	Sitting	.310	.154
Trunk	Child	Kneeling	.310	.133

TABLE 14. SUMMARY OF MAXIMUM POWER DENSITIES AND SARs CORRESPONDING TO 3.5-W INPUT POWER TO ANTENNA FOR VARIOUS EXPOSURE CONDITIONS

Antenna	Model	Position	Max Power density (mW/cm^2)	Max SAR (W/kg)
Roof	Woman	Leaning forward (43.5 cm)	.447	.081
Roof	Woman	Standing (63 cm)	.224	.171
Roof	Child	Leaning forward (39 cm)	.515	.182
Roof	Child (63 cm)	Standing	.224	.067
Trunk	Man	Standing (12 cm)	1.52	.420
Trunk	Woman	Standing (9.7 cm)	2.18	.700
Trunk	Child (15 cm)	Standing	1.25	.805
Trunk	Man	Sitting	.155	.077
Trunk	Child	Kneeling	.155	.067

half-wavelength dipole (Collin and Zucker 1969) resulted in the data shown in Tables 15 through 18. Tables 15 and 16 give the data for an antenna with 7-W, 835-MHz input power tabulated as a function of z and r in cylindrical coordinates with an origin at the center of the antenna. The location of each calculation is denoted by an asterisk spaced at intervals along the z and r axes of 10 cm in Table 15 and 5 cm in Table 16. Data for only one quadrant in a plane through the antenna are shown since the pattern is symmetrical with the remaining quadrants. The data tabulated above each asterisk correspond in descending order to the electric field strength in volts/meter, the magnetic field strength in amperes/meter, and the maximum equivalent power density in mW/cm^2 derived from either the magnetic or electric field, depending on which gives the highest value. In Tables 17 and 18 are presented similar data for 3.5 W input to the antenna.

In Table 19 is provided a direct comparison between maximum measured values and calculated theoretical values of power density. Some of the data compare closely, but other values differ up to a factor of two. The variations, probably due to antenna-automobile body interactions, are certainly within expectations.

We may conclude from the results that the mobile-antenna system can be operated safely well with all of the ANSI RFPG exposure guides in terms of both power density and maximum SAR for input powers of 3.5 W or less and within the guidelines of the ANSI exclusion clause for input powers up to 35 W. Furthermore, on the basis of average power density for the brief transmission periods in which persons may be exposed under the conditions studied in this research, operation of the antenna is not likely to result in emissions that exceed some of the newly proposed general population standards now being proposed by various government agencies for different tissue types and structures.

It has been shown that the experimental methods used in this research can adequately quantify both maximum exposure levels and SARs for subjects exposed in the near-field of UHF mobile transmitting antennas. These techniques can also be applied equally well to other exposure conditions, involving fixed portable and mobile antennas and radiation

TABLE 15. ELECTROMAGNETIC FIELDS AND EQUIVALENT POWER DENSITIES OF IDEAL DIPOLE ANTENNA, FREQ = 835.00 MHz, HEIGHT OR 1/2 LENGTH = 0.25 WAVELENGTHS, INPUT RESISTANCE = 72.00 OHMS, INPUT POWER = 7.00 WATTS, GRID SIZE = 0.10 m , ORIGIN (0.00, 0.00)

: LEGEND
: E (V/m)
: H (A/m)
: PD (mW/cm2)
: LOCATION = *

2.6591	3.4820	5.0882	6.6968	8.0539	9.0892	9.8081	10.2512
0.0000	0.0061	0.0118	0.0167	0.0207	0.0236	0.0257	0.0270
0.0019	0.0032	0.0069	0.0119	0.0172	0.0219	0.0255	0.0279
*	*	*	*	*	*	*	*
3.4868	4.5451	6.5659	8.4995	10.0220	11.0748	11.7050	11.9969
0.0000	0.0080	0.0152	0.0212	0.0257	0.0289	0.0307	0.0316
0.0032	0.0055	0.0114	0.0192	0.0266	0.0325	0.0363	0.0382
*	*	*	*	*	*	*	*
4.7747	6.1794	8.7705	11.0782	12.7036	13.6490	14.0501	14.0637
0.0000	0.0108	0.0204	0.0277	0.0327	0.0356	0.0370	0.0371
0.0060	0.0101	0.0204	0.0326	0.0428	0.0494	0.0524	0.0525
*	*	*	*	*	*	*	*
6.9457	8.8792	12.2391	14.8823	16.3958	16.9667	16.8984	16.4486
0.0000	0.0156	0.0285	0.0374	0.0424	0.0445	0.0446	0.0435
0.0128	0.0209	0.0397	0.0587	0.0713	0.0764	0.0757	0.0718
*	*	*	*	*	*	*	*
11.0601	13.8047	18.0452	20.6313	21.4516	21.1340	20.2282	19.0781
0.0000	0.0244	0.0424	0.0523	0.0559	0.0557	0.0535	0.0506
0.0324	0.0505	0.0864	0.1129	0.1221	0.1185	0.1085	0.0966
*	*	*	*	*	*	*	*
20.5094	24.1748	28.3645	29.2902	28.0923	26.0525	23.8488	21.7638
0.0000	0.0431	0.0678	0.0753	0.0739	0.0691	0.0634	0.0579
0.1116	0.1550	0.2134	0.2275	0.2093	0.1800	0.1515	0.1264
*	*	*	*	*	*	*	*
52.6234	50.7326	46.7358	41.2947	35.8521	31.1558	27.3031	24.1761
0.0000	0.0942	0.1164	0.1088	0.0956	0.0832	0.0729	0.0645
0.7345	0.6826	0.5793	0.4523	0.3445	0.2611	0.2003	0.1568
*	*	*	*	*	*	*	*
869.6282	116.2809	72.1078	53.9252	42.7597	35.2357	29.8747	25.8863
0.0000	0.2693	0.1960	0.1468	0.1156	0.0947	0.0800	0.0692
200.5811	3.5862	1.4488	0.8122	0.5034	0.3383	0.2415	0.1805
*	*	*	*	*	*	*	*
D	139.1818	85.3311	59.7408	45.6343	36.8271	30.8369	26.5088
D	0.4963	0.2481	0.1654	0.1241	0.0993	0.0827	0.0709
D	9.2856	2.3215	1.0318	0.5804	0.3714	0.2579	0.1895
*	*	*	*	*	*	*	*

TABLE 16. ELECTROMAGNETIC FIELDS AND EQUIVALENT POWER DENSITIES OF IDEAL DIPOLE ANTENNA, FREQ = 835.00 MHz, HEIGHT OR 1/2 LENGTH = 0.25 WAVELENGTHS, INPUT RESISTANCE = 72.00 OHMS, INPUT POWER = 7.00 WATTS, GRID SIZE = 0.05 m , ORIGIN (0.00, 0.00)

: LEGEND
: E (V/m)
: H (A/m)
: PD (mW/cm2)
: LOCATION = *

11.0601	11.8675	13.8047	16.0430	18.0452	19.5877	20.6313	21.2253
0.0000	0.0127	0.0244	0.0344	0.0424	0.0483	0.0523	0.0547
0.0324	0.0374	0.0505	0.0683	0.0864	0.1018	0.1129	0.1195
*	*	*	*	*	*	*	*
14.6845	15.6610	17.9361	20.4147	22.4414	23.8069	24.5375	24.7501
0.0000	0.0167	0.0318	0.0440	0.0531	0.0591	0.0626	0.0641
0.0572	0.0651	0.0853	0.1105	0.1336	0.1503	0.1597	0.1625
*	*	*	*	*	*	*	*
20.5094	21.6504	24.1748	26.6544	28.3645	29.1934	29.2902	28.8616
0.0000	0.0232	0.0431	0.0581	0.0678	0.0731	0.0753	0.0753
0.1116	0.1243	0.1550	0.1884	0.2134	0.2260	0.2275	0.2209
*	*	*	*	*	*	*	*
30.8711	31.9574	34.1058	35.7481	36.3288	35.9569	34.9261	33.5108
0.0000	0.0344	0.0617	0.0792	0.0882	0.0913	0.0908	0.0881
0.2528	0.2709	0.3085	0.3389	0.3500	0.3429	0.3235	0.2978
*	*	*	*	*	*	*	*
52.6234	52.0404	50.7326	48.9811	46.7358	44.1016	41.2947	38.5048
0.0000	0.0567	0.0942	0.1118	0.1164	0.1142	0.1088	0.1023
0.7345	0.7183	0.6826	0.6363	0.5793	0.5159	0.4523	0.3945
*	*	*	*	*	*	*	*
116.4322	98.6394	78.6102	67.0515	59.2884	53.1272	47.9189	43.4498
0.0000	0.1118	0.1558	0.1617	0.1534	0.1410	0.1283	0.1167
3.5956	2.5806	1.6390	1.1924	0.9323	0.7498	0.6209	0.5131
*	*	*	*	*	*	*	*
869.6282	210.8389	116.2809	87.2711	72.1078	61.7541	53.9252	47.7493
0.0000	0.2938	0.2693	0.2303	0.1960	0.1685	0.1468	0.1295
200.5811	11.7903	3.5862	2.0201	1.4488	1.0706	0.8122	0.6321
*	*	*	*	*	*	*	*
D	260.6218	138.9670	102.1752	81.7788	68.0898	58.1905	50.7132
D	0.7333	0.4200	0.2999	0.2330	0.1902	0.1604	0.1385
D	20.2722	6.6494	3.3909	2.0475	1.3634	0.9697	0.7234
*	*	*	*	*	*	*	*
D	181.9884	139.1818	107.0046	85.3311	70.4257	59.7408	51.7745
D	0.9925	0.4963	0.3309	0.2481	0.1985	0.1654	0.1418
D	37.1397	9.2856	4.1270	2.3215	1.4858	1.0318	0.7580
*	*	*	*	*	*	*	*

TABLE 17. ELECTROMAGNETIC FIELDS AND EQUIVALENT POWER DENSITIES OF IDEAL DIPOLE ANTENNA, FREQ = 835.00 MHz, HEIGHT OR 1/2 LENGTH = 0.25 WAVELENGTHS, INPUT RESISTANCE = 72.00 OHMS, INPUT POWER = 3.50 WATTS, GRID SIZE = 0.10 m , ORIGIN (0.00, 0.00)

: LEGEND
: E (V/m)
: H (A/m)
: PD (mW/cm2)
: LOCATION = *

1.8803	2.4622	3.5979	4.7353	5.6949	6.4270	6.9354	7.2487
0.0000	0.0043	0.0083	0.0118	0.0146	0.0167	0.0182	0.0191
0.0009	0.0016	0.0034	0.0059	0.0086	0.0110	0.0128	0.0139
*	*	*	*	*	*	*	*
2.4655	3.2139	4.6428	6.0101	7.0866	7.8311	8.2767	8.4831
0.0000	0.0056	0.0108	0.0150	0.0182	0.0204	0.0217	0.0224
0.0016	0.0027	0.0057	0.0096	0.0133	0.0163	0.0182	0.0191
*	*	*	*	*	*	*	*
3.3763	4.3695	6.2017	7.8335	8.9828	9.6513	9.9349	9.9445
0.0000	0.0077	0.0144	0.0196	0.0231	0.0252	0.0261	0.0263
0.0030	0.0051	0.0102	0.0163	0.0214	0.0247	0.0262	0.0262
*	*	*	*	*	*	*	*
4.9113	6.2786	8.6544	10.5234	11.5936	11.9973	11.9490	11.6309
0.0000	0.0110	0.0202	0.0265	0.0300	0.0314	0.0315	0.0308
0.0064	0.0105	0.0199	0.0294	0.0357	0.0382	0.0379	0.0359
*	*	*	*	*	*	*	*
7.8207	9.7614	12.7599	14.5885	15.1686	14.9440	14.3035	13.4903
0.0000	0.0172	0.0300	0.0370	0.0395	0.0394	0.0379	0.0358
0.0162	0.0253	0.0432	0.0564	0.0610	0.0592	0.0543	0.0483
*	*	*	*	*	*	*	*
14.5024	17.0942	20.0567	20.7113	19.8642	18.4219	16.8636	15.3893
0.0000	0.0305	0.0479	0.0532	0.0523	0.0488	0.0448	0.0409
0.0558	0.0775	0.1067	0.1138	0.1047	0.0900	0.0758	0.0632
*	*	*	*	*	*	*	*
37.2103	35.8734	33.0472	29.1997	25.3513	22.0305	19.3062	17.0951
0.0000	0.0666	0.0823	0.0769	0.0676	0.0588	0.0515	0.0456
0.3672	0.3413	0.2897	0.2261	0.1722	0.1305	0.1002	0.0784
*	*	*	*	*	*	*	*
614.9200	82.2230	50.9879	38.1309	30.2357	24.9154	21.1246	18.3044
0.0000	0.1904	0.1386	0.1038	0.0817	0.0670	0.0566	0.0489
100.2906	1.7931	0.7244	0.4061	0.2517	0.1691	0.1207	0.0902
*	*	*	*	*	*	*	*
D	98.4164	60.3382	42.2431	32.2684	26.0407	21.8050	18.7445
D	0.3509	0.1755	0.1170	0.0877	0.0702	0.0585	0.0501
D	4.6428	1.1607	0.5159	0.2902	0.1857	0.1290	0.0948
*	*	*	*	*	*	*	*

TABLE 18. ELECTROMAGNETIC FIELDS AND EQUIVALENT POWER DENSITIES OF IDEAL DIPOLE ANTENNA, FREQ = 835.00 MHz, HEIGHT OR 1/2 LENGTH = 0.25 WAVELENGTHS, INPUT RESISTANCE = 72.00 OHMS, INPUT POWER = 3.50 WATTS, GRID SIZE = 0.05 m , ORIGIN (0.00, 0.00)

: LEGEND
: E (V/m)
: H (A/m)
: PD (mW/cm2)
: LOCATION = *

7.8207	8.3916	9.7614	11.3441	12.7599	13.8506	14.5885	15.0085
0.0000	0.0090	0.0172	0.0243	0.0300	0.0341	0.0370	0.0387
0.0162	0.0187	0.0253	0.0341	0.0432	0.0509	0.0564	0.0597
*	*	*	*	*	*	*	*
10.3835	11.0740	12.6828	14.4353	15.8685	16.8340	17.3507	17.5009
0.0000	0.0118	0.0225	0.0311	0.0375	0.0418	0.0442	0.0453
0.0286	0.0325	0.0427	0.0553	0.0668	0.0752	0.0798	0.0812
*	*	*	*	*	*	*	*
14.5024	15.3091	17.0942	18.8475	20.0567	20.6428	20.7113	20.4083
0.0000	0.0164	0.0305	0.0411	0.0479	0.0517	0.0532	0.0532
0.0558	0.0622	0.0775	0.0942	0.1067	0.1130	0.1138	0.1105
*	*	*	*	*	*	*	*
21.8292	22.5973	24.1164	25.2777	25.6883	25.4254	24.6965	23.6957
0.0000	0.0243	0.0436	0.0560	0.0624	0.0646	0.0642	0.0623
0.1264	0.1354	0.1543	0.1695	0.1750	0.1715	0.1618	0.1489
*	*	*	*	*	*	*	*
37.2103	36.7981	35.8734	34.6349	33.0472	31.1846	29.1997	27.2270
0.0000	0.0401	0.0666	0.0791	0.0823	0.0807	0.0769	0.0723
0.3672	0.3591	0.3413	0.3182	0.2897	0.2579	0.2261	0.1972
*	*	*	*	*	*	*	*
82.3300	69.7486	55.5858	47.4126	41.9232	37.5666	33.8838	30.7237
0.0000	0.0790	0.1102	0.1143	0.1085	0.0997	0.0907	0.0825
1.7978	1.2903	0.8195	0.5962	0.4662	0.3749	0.3104	0.2565
*	*	*	*	*	*	*	*
614.9200	149.0856	82.2230	61.7100	50.9879	43.6668	38.1309	33.7639
0.0000	0.2078	0.1904	0.1628	0.1386	0.1192	0.1038	0.0916
100.2906	5.8951	1.7931	1.0100	0.7244	0.5353	0.4061	0.3161
*	*	*	*	*	*	*	*
D	184.2875	98.2645	72.2488	57.8263	48.1468	41.1469	35.8597
D	0.5185	0.2970	0.2121	0.1648	0.1345	0.1134	0.0979
D	10.1361	3.3247	1.6954	1.0238	0.6817	0.4848	0.3617
*	*	*	*	*	*	*	*
D	128.6853	98.4164	75.6637	60.3382	49.7985	42.2431	36.6101
D	0.7018	0.3509	0.2339	0.1755	0.1404	0.1170	0.1003
D	18.5698	4.6428	2.0635	1.1607	0.7429	0.5159	0.3790
*	*	*	*	*	*	*	*

devices operating at other frequencies. It appears that the methodology would be most useful in determining whether certain types of radiating devices could meet the ANSI 0.4-W/kg average and 8.0-W/kg maximum SAR exclusion clause. The models used in this research were simple, homogeneous figures, but there are no technical restrictions in fabricating more advanced and realistic designs.

TABLE. 19. COMPARISON OF MEASURED MAXIMUM POWER DENSITIES FROM MOBILE ANTENNA WITH CALCULATED MAXIMUM THEORETICAL VALUES FROM HALF-WAVELENGTH-LONG DIPOLE WITH 1-W INPUT TO ANTENNA

			Maximum Power Density (mW/cm^2)		
Mobile Antenna	Model	Position	H field derived	E field derived	measured
Roof	Woman	Leaning forward (43.5 cm)	.0701	.0672	0.128
Roof	Woman	Standing (63 cm)	.0334	.0328	0.0639
Roof	Child	Leaning forward (39 cm)	.872	.0828	0.1475
Roof	Child	Standing (63 cm)	.0334	.0328	0.0639
Trunk	Man	Standing (12 cm)	.921	.590	0.435
Trunk	Woman	Standing (9.7 cm)	1.41	.759	0.624
Trunk	Child	Standing (15 cm)	.590	.434	0.357

REFERENCES

ANSI (1982):. "American National Standard safety levels with respect to human exposure to radio frequency electromagnetic fields, 300 kHz to 100 GHz". American National Standards Institute, Institute of Electrical and Electronics Engineers, Inc.

Carpenter RL, Ferri ES, Hagan GL (1974): Assessing microwaves as a hazard to the eye - progress and problems. Proc of Int Symp on Biologic Effects and Health Hazards of Microwave Radiation. Warsaw: Polish Medical Publishers, pp. 178-185.

Collin RE, Zucker FJ (1969): Antenna theory. New York: McGraw-Hill, Part I, p. 367.

Guy AW (1971): Analysis of electromagnetic fields induced in biological tissues by thermographic studies on equivalent phantom models. IEEE Trans MTT-19:205-214.

Guy AW, Kramar PO, Harris CA, Chou CK (1980): Long-term 2450 MHz CW microwave irradiation of rabbits: Methodology and evaluation of ocular and physiologic effects. J Microwave Power 15:37-44.

Guy AW, Lin JC, Kramar PO, Emery AF (1975): Effect of 2450-MHz radiation on the rabbit eye. IEEE Trans MTT-23:492-498.

Guy AW, Webb MD, McDougall JA (1976a): Assessment of the EM field coupling of 915 MHz oven door leakage to human subjects by thermographic studies on equivalent phantom models. General Electric Company, Louisville, Kentucky, Scientific Report #7.

Guy AW, Webb MD, Sorensen CC (1976b): Determination of power absorption in man exposed to high frequency electromagnetic fields by thermographic measurements of scale models. IEEE Trans BME-23:361-371.

Kramar PO, Emery AF, Guy AW, Lin JC (1975): The ocular effects of microwaves on hypothermic rabbits: A study of microwave cataractogenic mechanisms. NY Acad Sci 247:155-165.

Kramar PO, Harris C, Emery AF, Guy AW (1978): Acute microwave radiation and cataract formation in rabbits and monkeys. J Microwave Power 13(3):240-249.

McAfee RD, Longacre AJ, Bishop RR, Elder ST, May JG, Holland MG (1979): Absence of ocular pathology after repeated exposure of unanethesized monkeys to 9.3 GHz microwaves. J Microwave Power 14:41-44.

APPENDIX A

COMPUTERIZED THERMOGRAPHIC SYSTEM

An interactive computer approach to the thermographic recording analysis was implemented for assessing the SAR distribution. In Fig. 1 is diagrammed the system used for thermographic work. The AGA thermovision 680 system was interfaced with an AGA-supplied, Oscar digitizer-digital tape-recording system. The system was used to digitize and store thermographic images as well as to provide interfacing to a computer. Images could be recorded at will or recorded automatically over a selected sampling interval. Once recorded, the images could either be played back and analyzed on the thermography system with all of its analog data processing features, or they could be transferred to a digital tape (Fig. 2) and then to a computer (Fig. 3). When the digital tape-recording system was interfaced with a PDP-11/34 computer, its graphics terminal and plotter (Fig. 4) were used to print the dosimetry thermograms after analysis. Magnetic tape from the thermograph laboratory was transported to the computer room for general image processing by special software. The software was developed for detailed computer-image analysis. The analysis system was semi-interactive, enabling the operator to identify exactly the regions in which images were of interest. Once these regions were defined, a 12-parameter intraregional statistical analysis could be made. The operator could then determine in any selected region the highest SAR value, lowest value, range, median, average, variance, skewness of distribution, area of region, parameter, shape factor, geometric centroid, and percentage of total image observed. The software was arranged to enable tailoring to specific applications by selection and elimination of various subroutines. Algorithms were added to enable the computer to perform automatic interpretation and analysis. This system significantly accelerated the thermographic analysis of SAR distribution patterns and provided greater reliability of data.

The graphics system employed the Hewlett/Packard 7220 flatbed plotter and the Qume Sprint-5 printer. Both served as peripherals to the PDP-11/34 minicomputer. The HP plotter output consisted of four basic plot types: gray-scale, contour, multiple-profile, and single-profile scans. The Qume output consisted of gray-scale printouts showing the different areas of heating as varying shades of gray.

An example of the contour plot is presented in Fig. 5; this plot corresponds to a close-up, midbody plot of the thermogram shown in Fig. 6, which was taken directly from the thermograph image indicator. Each curve in the contour plot is an iso-SAR line showing points of equal SAR in the thermographed object. Up to 20 different contour levels may be included in a single plot, although only six are shown in the example. Additionally, the contours are plotted in a sequence of four colors for simplification of identification of isothermal lines. The colors are not visible in the example, owing to the photocopying process; this disadvantage was the primary consideration in not using this plot type in this report. In Fig. 5, contours at equal intervals cover the range of SAR values from 0.05 to 0.390 W/kg per mW/cm^2. In Fig. 6(b) is reproduced a processed gray-scale plot of the body midsection, and the scans reproduced in Fig. 6(c) show the SARs along specific scan lines in the digitized thermograph. Each thermograph is made up of 128 scan lines. All B-scan plots were labeled to indicate the proper point of comparison with a gray-scale plot of the same image. Profile plots were composed of multiple B-scans, as shown in Fig. 6(d). These plots presented SAR over the thermographed object in relief. The profile plots included later in this section show the entire image for all exposures and closeup scans for some exposures. The plot could be limited to any rectangular area of the image; thus the analyst could blowup areas of interest for more detailed examination. Gray-scale plots were printouts displaying heating as eight different shades; each shade of gray represented a specific heating (SAR) range. The SAR ranges were displayed at the bottom of each plot as shown in Fig. 6(b). For each exposure the user could also display in terms of temperature, temperature change, SAR, or current density.